

Article

Spectral Analysis of Anomalous Capacitance Measurements in Interleaving Structures: Study of Frequency Distribution in Photomultipliers

Víctor Milián-Sánchez ¹, Miguel E. Iglesias-Martínez ^{2,3,*}, Jose Guerra Carmenate ²,
Juan Carlos Castro-Palacio ^{2,4}, Eduardo Balvis Outeiriño ⁵, Pedro Fernández de Córdoba ²,
Francisco Misael Muñoz-Pérez ⁴, Juan Antonio Monsoriu ⁴ and Sarira Sahu ⁶

- ¹ Institute for Industrial, Radiophysical and Environmental Safety, Universitat Politècnica de València, Camino de Vera, s/n, 46022 Valencia, Spain; vicmisan@iqn.upv.es
 - ² Grupo de Modelización Interdisciplinar, InterTech, Instituto Universitario de Matemática Pura y Aplicada, Universitat Politècnica de València, Camino de Vera, s/n, 46022 Valencia, Spain; jguecar@doctor.upv.es (J.G.C.); juancas@upvnet.upv.es (J.C.C.-P.); pfernandez@mat.upv.es (P.F.d.C.)
 - ³ Grupo de Ingeniería Física, Escuela de Ingeniería Aeronáutica y del Espacio, Universidad de Vigo, Edif. Manuel Martínez Risco, Campus de As Lagoas, 32004 Ourense, Spain
 - ⁴ Centro de Tecnologías Físicas, Universitat Politècnica de València, Camino de Vera, s/n, 46022 Valencia, Spain; fmmuope1@upvnet.upv.es (F.M.M.-P.); jmonsori@fis.upv.es (J.A.M.)
 - ⁵ Departamento de Ingeniería de Sistemas y Automática, Escuela Superior de Ingeniería Informática, Universidade de Vigo, Edificio Politécnico s/n, 32004 Ourense, Spain; ebalvis@uvigo.es
 - ⁶ Instituto de Ciencias Nucleares, Universidad Autónoma de México, Circuito Exterior, C.U., A. Postal 70-543, Mexico City 04510, Mexico; sarira@nucleares.unam.mx
- * Correspondence: miigmar@upv.es



Citation: Milián-Sánchez, V.; Iglesias-Martínez, M.E.; Carmenate, J.G.; Castro-Palacio, J.C.; Outeiriño, E.B.; Fernández de Córdoba, P.; Muñoz-Pérez, F.M.; Monsoriu, J.A.; Sahu, S. Spectral Analysis of Anomalous Capacitance Measurements in Interleaving Structures: Study of Frequency Distribution in Photomultipliers. *Symmetry* **2024**, *16*, 15. <https://doi.org/10.3390/sym16010015>

Academic Editor: Marek T. Malinowski

Received: 18 October 2023
Revised: 10 December 2023
Accepted: 15 December 2023
Published: 21 December 2023



Copyright: © 2023 by the authors. Licensee MDPI, Basel, Switzerland. This article is an open access article distributed under the terms and conditions of the Creative Commons Attribution (CC BY) license (<https://creativecommons.org/licenses/by/4.0/>).

Abstract: This study presents experimental results on capacitance fluctuations in several devices located within an interleaving structure. Specifically, it examines the behavior of the capacitance between the anode and cathode of a photomultiplier, comparing it with the characteristics of the ultra-stable capacitor analyzed in via measurements inside and outside a modified Faraday cage. The results cover spectral and correlation analyses both inside and outside the box, confirming differences in the spectrum using the periodograms. In particular, the confidence intervals for the mean capacitance values show significant changes between the two scenarios, from the inside to the outside of the enclosure. In the case of the ultra-stable capacitor, there is an increase from 0.004 to 0.008 nF. On the other hand, a symmetry analysis is conducted for all measurements taken both outside and inside the modified Faraday cage. It is observed that in all cases, there is clear non-symmetric behavior in the data.

Keywords: spectral analysis; interleaving structures; capacitance

1. Introduction

The primary purpose of a Faraday cage is to mitigate the influence of electromagnetic radiation and reduce noise, making it a crucial component in electromagnetic compatibility testing models. However, when alternating layers of conductive and non-conductive materials are employed to create periodic structures, intriguing anomalies manifest in the measurements obtained using various instruments [1,2].

Interleaving structures involve the alternation of distinct conductive and insulating layers in a well-defined pattern. Such configurations are commonly found in multilayered printed circuit boards, microelectromechanical systems (MEMS), and integrated circuits, among other applications [3,4]. Conventionally, capacitance between conductive elements separated by an insulating layer can be predicted using standard equations, primarily based on geometric factors and material properties. However, recent investigations have

revealed deviations from these predictions, sparking a quest to comprehend the underlying mechanisms responsible for the observed anomalies [5].

The analysis of frequency-dependent capacitance measurements in layered structures has been the focus of several studies. In [6], an analysis is presented based on equilibrium dynamical fluctuations of electrode charge in constant-potential molecular simulations. This study extends a fluctuation–dissipation relation for capacitance, particularly in the low-frequency limit. The work provides an illustration using water–gold nanocapacitors. Another contribution, found in [7], demonstrates the spectral dependence based on the material composition of the structure, employing impedance spectroscopy methods.

Furthermore, in [8], additional insights are provided via a review of planar magnetics and structures designed to reduce parasitic elements and enhance efficiency. This review encompasses various strategies and technologies aimed at optimizing the performance of layered structures in terms of capacitance and overall electrical characteristics.

These works collectively contribute to the understanding of frequency-dependent capacitance in layered structures, offering valuable insights into material-dependent behaviors and potential enhancements in efficiency.

Figure 1 illustrates a notable example of this variability, where the measured capacitance deviated from the design value ($C_0 = 10.1936$ nF). The observed fluctuations exceeded the uncertainty intervals of the means, specifically fluctuating between -0.18% and $+0.18\%$ of the specified value (i.e., ranging from 10.1758 to 10.2117 nF). In this experiment, the applied signal was 1 Vac, and the frequency was 100 Hz. The uncertainty limits given by Fischer LSD intervals are also represented.

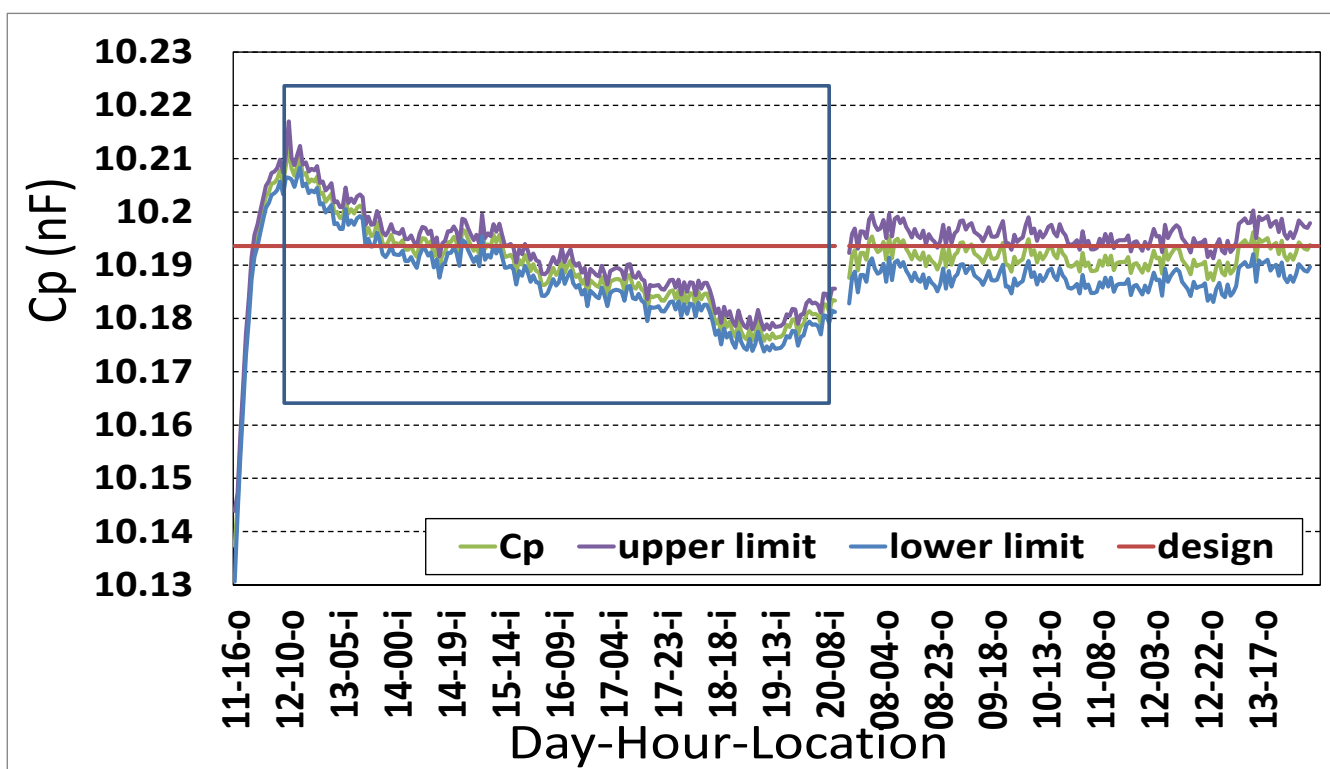


Figure 1. Capacitance fluctuations above and below the actual value, 10.1936 nF. The lower values at the left-hand side were recorded outside the box (at 100 Hz) after having been inside the cage for three weeks at the frequency of 10 kHz. The highlighted region was recorded inside the box, and in the right-hand side region, C_p slowly recovers its design values after being placed outside the enclosure. The mean amplitude of the confidence intervals of the means was 0.004 nF in the two first time intervals, whereas it was 0.008 nF in the third interval.

The capacitance at 100 Hz was 10.1936 nF with standard deviation $\sigma_1 = 0.001654$ nF, whereas at 10 kHz, it was 10.0766 nF and $\sigma_2 = 0.000123$ nF, and the capacitance changes occurred immediately after changing the frequency. But these kinds of responses were not the same when the capacitor was tested inside the box during the three preceding weeks at 10 kHz, and it was shown that capacitance ranged between 10.0745 nF and 10.0770 nF (see also Figure 9a in [5]). After that, the capacitance was extracted from the cage and measured at 100 Hz (see the left-hand side of the highlighted region): it is apparent that the capacitance did not change immediately to 10.1936 nF and reached values lower than 10.1400 nF despite being measured at 100 Hz. This value was very much below its actual value of 10.1936 nF (at 100 Hz). It clearly shows not only that the capacitor had reached even lower values than 10.14 nF (when working a 10 kHz) but that after its extraction, it was slowly rising to its actual value of 10.1936 nF.

In other words, the capacitor remained in this situation of lower capacitance despite being extracted from the enclosure (at a frequency of 100 Hz) but was returning slowly to values closer to its actual design value. Afterward, when placed inside the box, it experienced oscillations as shown in the highlighted region, and later, after its subsequent extraction from the box, it returned slowly to its design value and remained stable for weeks. Moreover, the confidence level of de means was ± 0.002 nF in the first- and second-time intervals, whereas it increased to ± 0.004 nF in the third interval.

In addition, it was found that the above-referred changes sometimes correlated (although moderately) with space weather indices, namely (i) the geomagnetic activity, GMA, which is, in turn, quantified using the parameter Dcx, and/or (ii) with the cosmic ray activity (CRA), which was captured using the cosmic ray induced neutron (CRN) count data (defined as N). Since there was no model for explaining those results, it was first intended to find some order in the puzzling results: for this purpose, and as a first step, we tried to find out the circumstances under which those variations were correlated with the independent variables GMA and/or with CRA.

Later, using a toy model, it was considered that the relative humidity (RH) should not be underestimated [9–11]. Thus, based on this observation, we added as a new variable the relative humidity, but the one measured inside the box and nearby the device under test (DUT). This procedure was applied in a recent work about the response of a coil inside one of those periodic structures [12]. By this means, the inductance of a coil turned out to be correlated with two variables, namely temperature T and RH, with a correlation coefficient of 95%. This result raised the question of whether low humidity values (less than 60%) could determine the value of the inductance, and whether it had to be also considered in the case of a capacitor.

Consequently, it turned out to be necessary to modify the experimental setup and to repeat some previous capacitance measurements by adding measurements of both temperature T and relative humidity RH just beside the DUT.

This repetition of the experiment was also intended to answer some questions such as (a) if these results would be similar if the structure of the box changed and (b) if the capacitance would experience similar variations if the dielectric of the capacitor was replaced by a vacuum tube. With respect to question (a), this work shows the results of measurements carried out in the period April–September 2020, which show that capacitance variations could also be detected within a cage with a different structure and that they were also correlated with space weather factors. As the first relevant result, it is obtained that the spectra, inside and outside the Faraday box, are quite different.

Furthermore, as a complement to the previous experiment, the response of a photomultiplier (PMT) was also tested.

Finally, since the discovery of radioactivity, there has always been a keen interest in the possibility of altering nuclear decay processes and in the search for natural or artificial mechanisms that could bring about such changes. Over the past century, potential factors responsible for introducing variations and perturbations in the measurement of nuclear decay rates have been repeatedly scrutinized [13–15]. This research originated from the

analysis of decay rate measurements of various nuclides using a Geiger–Müller counter tube within a modified Faraday cage (MFC). This MFC, resembling a typical Faraday cage, featured modifications on all sides via the addition of alternating metal and organic material sheets [1].

In recent studies, works such as [16–18] have delved into examining the use of machine learning methods, the predictive behavior of the influence exerted by active devices, and organic compounds on the measurement of physical variables. These investigations aim to elucidate the impact of active devices and organic compounds on the accuracy and reliability of physical measurements, shedding light on potential correlations and providing valuable insights into the interaction dynamics between these elements and the measured variables. The exploration of these relationships contributes to a deeper understanding of the underlying mechanisms, fostering advancements in the field of physical measurements and sensor technologies [19,20].

The observed unusual results raised questions about the potential impact on the circuitry of nuclear instrumentation when measuring within such a structure and the need for a comprehensive explanation.

The main novelty of this study lies in its detailed experimental approach to capacitance fluctuations in devices located within an interleaving structure. Specifically, it examines the behavior of capacitance between the anode and cathode of a photomultiplier, comparing it with the characteristics of the previously analyzed ultra-stable capacitor. The results reveal significant differences in the spectrum and mean capacitance values inside and outside the enclosure, providing a deeper understanding of how the environment affects these measurements. This experimental approach and the derived conclusions contribute to the overall understanding of capacitance fluctuations in various contexts.

The work has been organized as follows: Section 2 presents the materials and methods used in the research. Section 3 presents the obtained results from the experiments carried out, and Section 4 shows a discussion of the experimental results. Finally, the conclusions of the work are presented in Section 5.

2. Materials and Methods: Capacitance Variability Reproducibility

The procedures used in the experiments presented in this work are the same as in the previous papers [5,12], but different enclosures were used, as well as the locations where T and RH were measured. The experiment with the 10 nF capacitance (E.I) was performed using three boxes: one $0.5 \times 0.5 \times 0.5 \text{ m}^3$ external MFC built with four alternating layers of aluminum and self-adhesive elastomeric material. Inside this cage, a second box was placed, built with galvanized steel and cork sheeting, and inside this second box, a third one was used.

The latter was a carton box surrounded by a metallic grid. The capacitor was placed in the center of this structure to avoid inductances between them and the metallic components of the enclosure. The aim of this change in the number of shields was to check whether such enclosures would cause significant variations in the measurements. In addition, the experiment was carried out at a time of minimum solar activity, as was the case in the summer of 2020. The results are presented in Section 3.

In the experiment with the photomultiplier (E.II), only one cage of $0.5 \times 0.5 \times 0.5 \text{ m}^3$ dimensions and four alternating layers of aluminum and cork sheeting was used.

The experiments with the vacuum (E.III) tubes were carried out only with the external box used in (E.I), and the temperature and RH sensors were placed near the DUT.

As a means of analyzing spectral patterns, this work proposes the use of the periodogram. The periodogram is a fundamental tool in the analysis of signals and time series. Next, we will explore how the periodogram can be used in this context.

The tests were conducted with temperatures ranging between 27.1 and 30.9 degrees Celsius [12].

The measurements on the photomultiplier tube (PMT) were specifically conducted to analyze its capacitance fluctuations within the interleaving structure. While we acknowl-

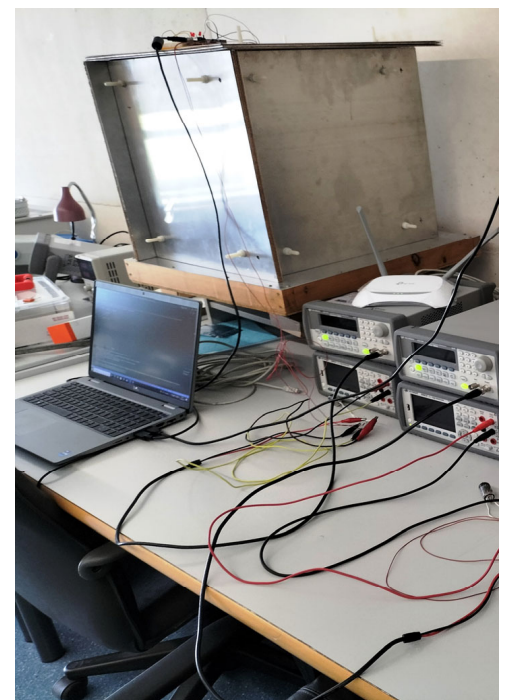
edge the primary operational function of a PMT in converting photons into an electrical signal, our focus in this study is directed toward understanding the capacitance behavior of the PMT when placed within the proposed experimental setup.

The choice of the photomultiplier in our research was motivated by its relevance in electronic applications and the potential impact of its capacitance characteristics on overall performance.

Figure 2 depicts the illustration of the modified Faraday cage (Figure 2a) and the test bench used for conducting the experiments (Figure 2b). The modified Faraday cage serves as a controlled environment, isolating the devices from external electromagnetic influences. On the other hand, the test bench represents the experimental setup designed to measure and analyze capacitance fluctuations within the devices placed inside the modified Faraday cage.



(a)



(b)

Figure 2. Illustration of (a) modified Faraday cage; (b) test bench for the experiments.

2.1. Correlations and Periodograms

For finite duration, discrete-time signals $\{x(n)\}_{n=0}^{M-1}$ (which represent the signal to be processed), and a sample of length M , the classic method for estimation of the power spectrum is the periodogram. The periodogram is defined by (1) as follows:

$$P_{xx}(f) = \frac{1}{M} \left| \sum_{n=0}^{M-1} x(n) e^{j2\pi f_n n} \right|^2 \quad (1)$$

where f_n is the instantaneous frequency of the signal to be processed and $P_{xx}(f)$ is the amplitude power spectrum of the response times vector. The spectrum-based analysis is used as a supplement to the calculation of spectral entropy [19–22].

2.2. Photomultiplier Anode to Cathode Capacitance Variability inside an MFC

In a previous work [5], it was observed that the spectrum of a Cs-137 source changed when placed inside the box. So, to check the possible variability of the circuitry of a PMT again, capacitance measurements were performed between the cathode and anode of the device. The circuitry consists of a combination of the capacitances of the voltage divisor and the capacitance between the anode and cathode.

The capacitance between the two mentioned electrodes of a commercial PMT, when measured outside and inside the box, can be represented by $C_{PMT,o}$ and $C_{PMT,i}$, respectively. The measurement results obtained both inside (IN) and outside (OUT) are presented in Figure 3.

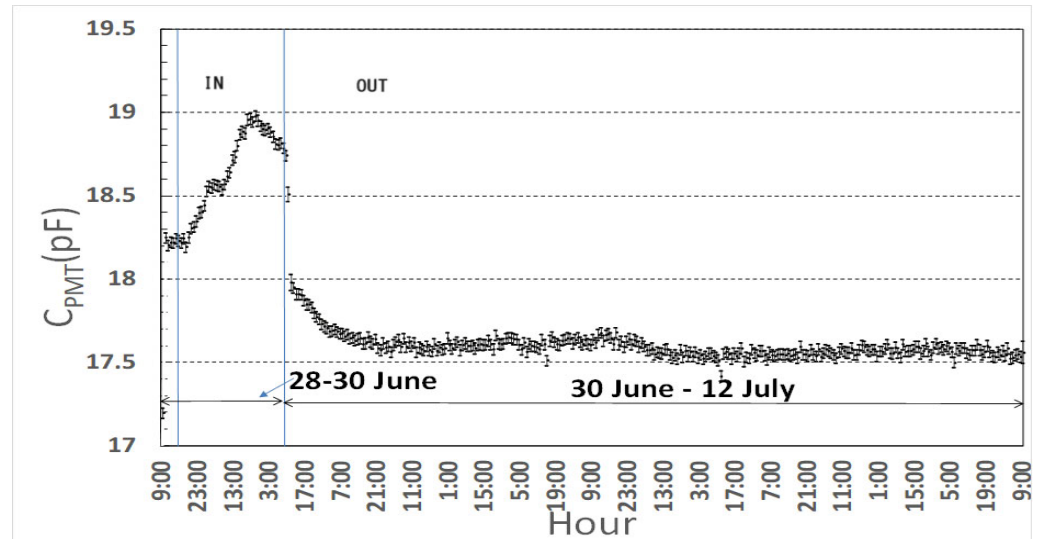


Figure 3. Capacitance measurements of the anode–cathode photomultiplier recorded both inside and outside the enclosure. IN refers to $C_{PMT,i}$ measurements taken within the enclosure from “28–30” June 2016. An observed lag effect occurred when the photomultiplier was removed from the enclosure and placed outside (OUT). Subsequently, the capacitance remained stable.

The measurements show again that the capacitance changes significantly with time inside the box, but it is very stable outside. In this way, it was shown that one could expect anomalous results when analyzing the spectrum of a sample.

In Figure 4, the schematic model of the design flux is shown. This outline reflects the structure and key findings of the study on capacitance fluctuations in devices within an interleaving structure, highlighting the comparison between the photomultiplier and the ultra-stable capacitor, as well as the influence of the environment on the measurements.

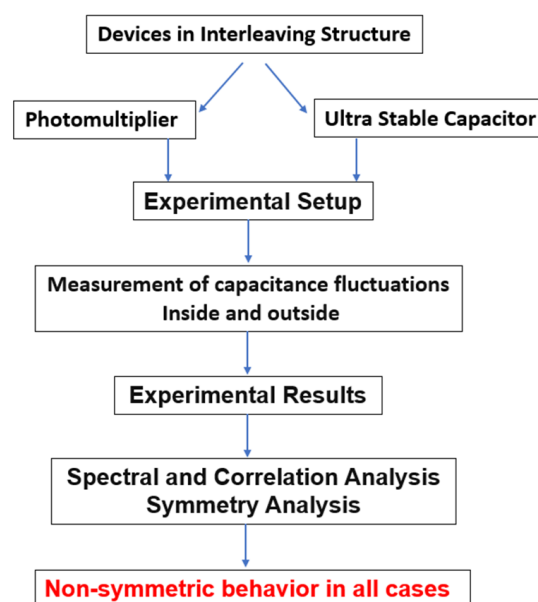


Figure 4. Schematic model of the design flux for the experiments.

3. Results

3.1. Capacitance Measurements during April–September 2020

To try to quantify the described capacitor responses based on the spectral analysis, periodograms of the capacitance measurements were performed. Figure 5a,b, respectively, show the obtained results. It is remarkable that the distribution of power into frequency components changes when capacitance measurements over time are taken outside and inside the box, respectively.

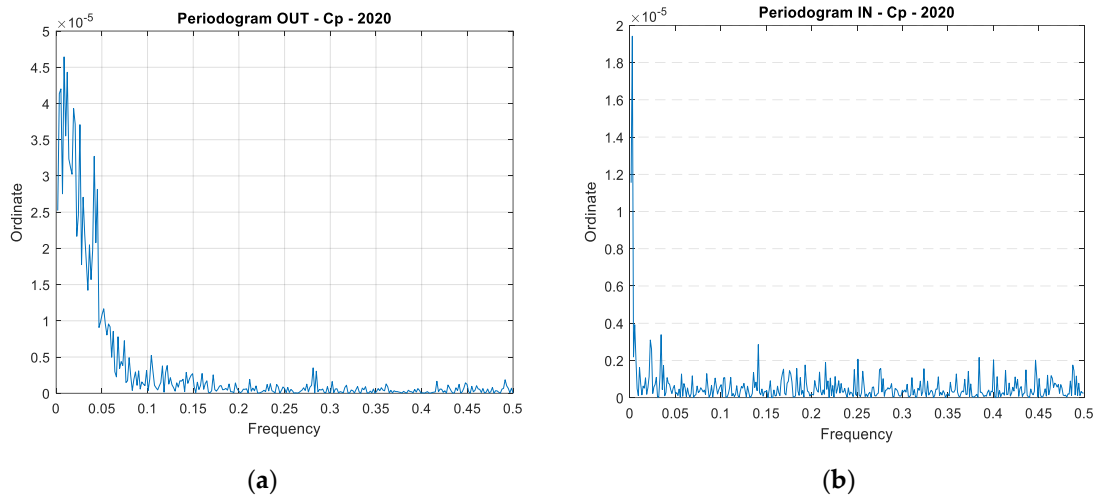


Figure 5. Periodograms for (a) capacitance time series outside the box for measurements made between 4–27 July 2020; (b) capacitance time series inside the box for measurements made between 28 July 2020 and 8 September 2020.

As depicted in Figure 5, the spectrum exhibits distinct peaks but is also subject to the influence of noise and artifacts within the data. The presence of noise or the occurrence of artifacts, evident in the fluctuations in measurements, can introduce randomness into the periodogram. These elements may inadvertently give rise to undesirable frequency components that impact the integrity of the useful frequency information.

We analyze the periodogram of the geomagnetic activity (Dcx) for the same period of the measurements carried out inside and outside the Faraday box; the obtained results are shown in Figure 6.

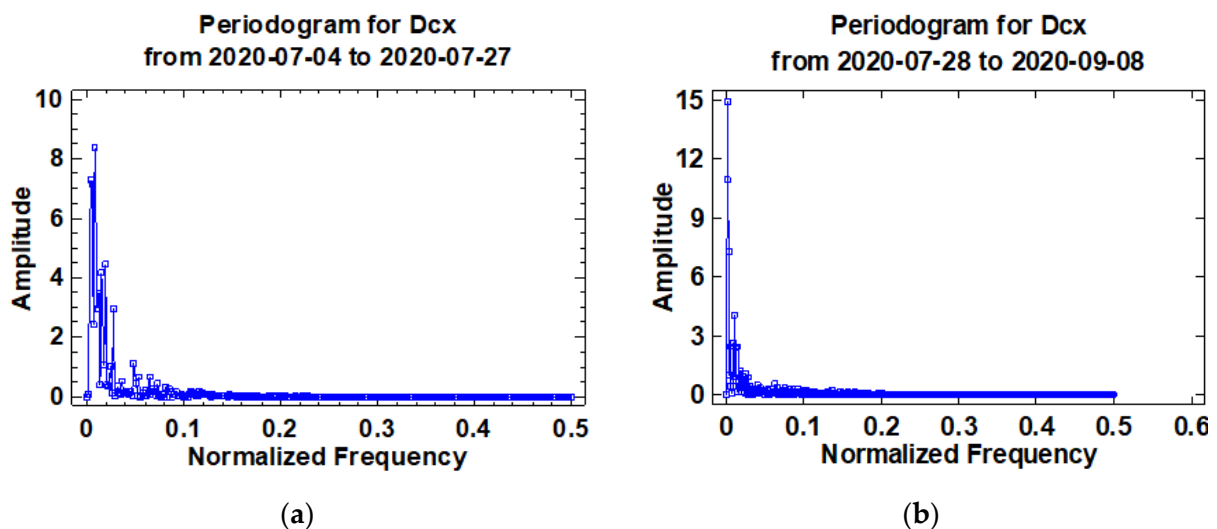


Figure 6. Periodograms for (a) Dcx for the same period as in Figure 5a; (b) Dcx for the same period as in Figure 5b.

3.2. Measurements in a Photomultiplier inside an MFC

The last point refers to the correlations between space weather parameters [5] and the variability of C_{PMT} . Since one can consider that the variability of the capacitance is proportional to the variability of the permittivity ϵ_x of the dielectric x , the variability of the capacitance inside the box can be considered proportional to $\Delta\epsilon'_x$, where the prime refers to the inside. So, one can analyze the correlation between $\Delta\epsilon'_x$ and Dcx (as shown in Figure 7a) and between $\Delta\epsilon'_x$ and N (Figure 7b).

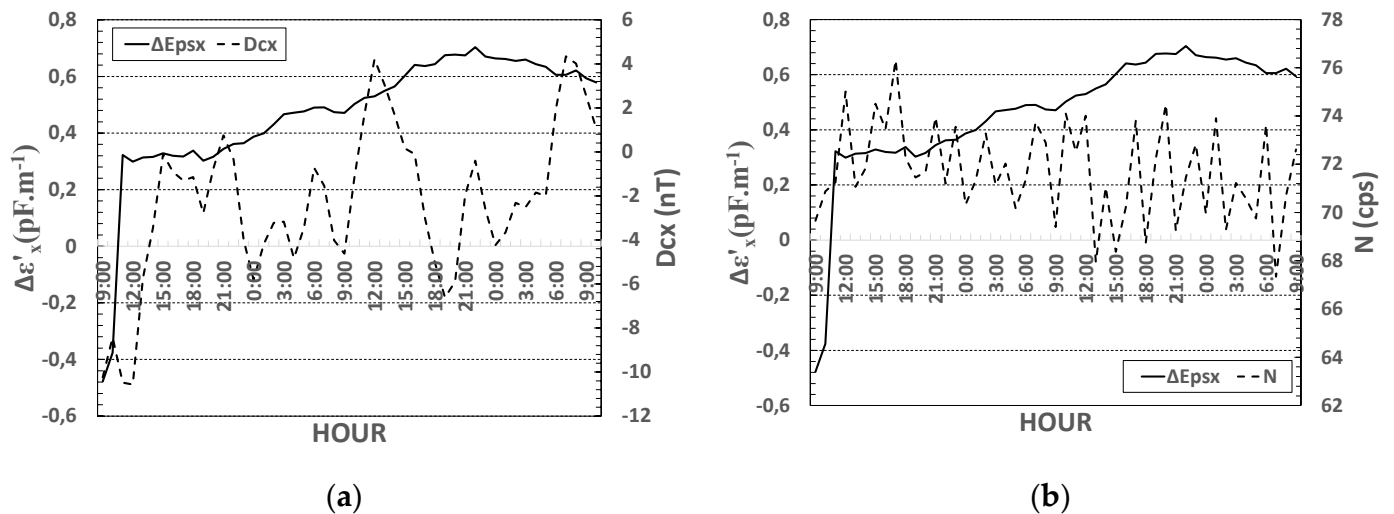


Figure 7. Comparison of $\Delta\epsilon'_x$ with Dcx and with N : (a) Graphs $\Delta\epsilon'_x$ and Dcx are correlated. (b) Graphs $\Delta\epsilon'_x$ and N are not correlated. However, there is a moderate result for the multiple regression analysis.

The jump of $\Delta\epsilon'_x$ appears to happen at the same time as the jumps of Dcx and N . These correlations are significant in the case of Figure 8a and not significant in Figure 8b; but a multiple regression analysis yields a moderate correlation between $\Delta\epsilon'_x$ and the two variables Dcx and N (p -value = 0.0039 and $R^2 = 21.4\%$). These results are presented in Table 1.

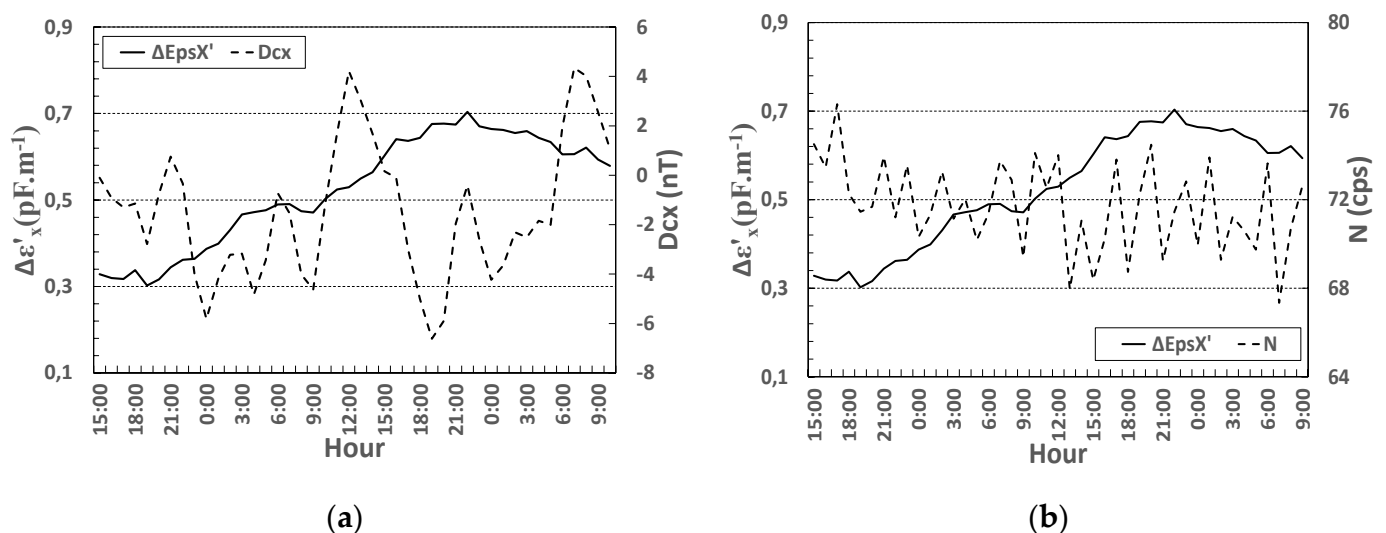


Figure 8. In (a,b), it is analyzed what happens when the jump is excluded from the analysis. In this case, there is an inverse correlation only between $\Delta\epsilon'_x$ and N (in d).

Table 1. Correlation between the analyzed variables ($\Delta\epsilon'_x$, Dcx, N).

Correlations Indexes between $\Delta\epsilon'_x$ and Cosmic Weather Variables (Dcx, N)			
	$\Delta\epsilon'_x$ –Dcx <i>p</i> -Value Pearson Coefficient	$\Delta\epsilon'_x$ –N <i>p</i> -Value Pearson Coefficient	$\Delta\epsilon'_x$ –(Dcx,N) <i>p</i> -Value R ²
Jump included	0.0009 0.461	0.6525 > 0.05 −0.066	0.0039 21.4%
Jump excluded	0.93 > 0.05 0.0133	0.026 −0.3393	0.0864 > 0.05 11.5%

We also search for correlations in those parts of the curves just after the jump. Here it can be seen that the result of the correlation analyses matches with one of the observations performed in [8]. In that paper, it was intended to derive under which circumstances one could observe correlations between decay rates and Dcx and/or N. In Table 1, the correlations between the considered variables are presented (Pearson's correlation coefficients show a correlation between $\Delta\epsilon'_x$ and N in those parts of the curves just after the jump).

3.3. Asymmetry Analysis

In this section, we conducted asymmetry analyses both inside and outside the MFC. The aim of these analyses was to assess and compare the signal's behavior in both situations. The MFC provided an environment with electromagnetic shielding properties, enabling an exploration of the influence of external factors on the signals within the photomultiplier. Furthermore, in this study, the skewness coefficient served as a key analytical tool. The skewness coefficient was employed to quantify and measure the degree of asymmetry in the data distributions obtained both inside and outside the cage. This statistical metric allowed for an objective evaluation of the symmetry or asymmetry of the data distributions, contributing to understanding the impact of the MFC on the shape and behavior of the photomultiplier's signal. Table 2 presents a summary of the skewness coefficient calculation both outside and inside the cage.

Table 2. Skewness coefficients for the data in Figure 3.

Data from Figure 2 Skewness Values	
Inside	−2.2168
Outside	2.1978

Similarly, Figure 9 displays a representative collection of histograms depicting the measurements conducted on the time series presented in Figure 4. These histograms vividly portray the asymmetry present in each distribution. In each graph, a comparison was drawn by superimposing a normal distribution, and the outcomes align with the data detailed in Table 2, illustrating the Skewness values of the time series both within and outside the enclosure. This reinforces the coherence of the findings, providing additional support to the consistency of the results.

The graphical representation shown in Figure 9 is based on the asymmetry observed in each time series of Figure 3, both inside and outside the Faraday cage. Asymmetry, in this context, refers to the disparity in the distribution of data around its mean. By examining the histograms, we can visualize how the presence of the Faraday cage affects the data distribution, providing a clear insight into the quantitative differences in asymmetry inside and outside the mentioned cage. The red line is just a reference to compare the probability distribution of the histogram with a Gaussian distribution.

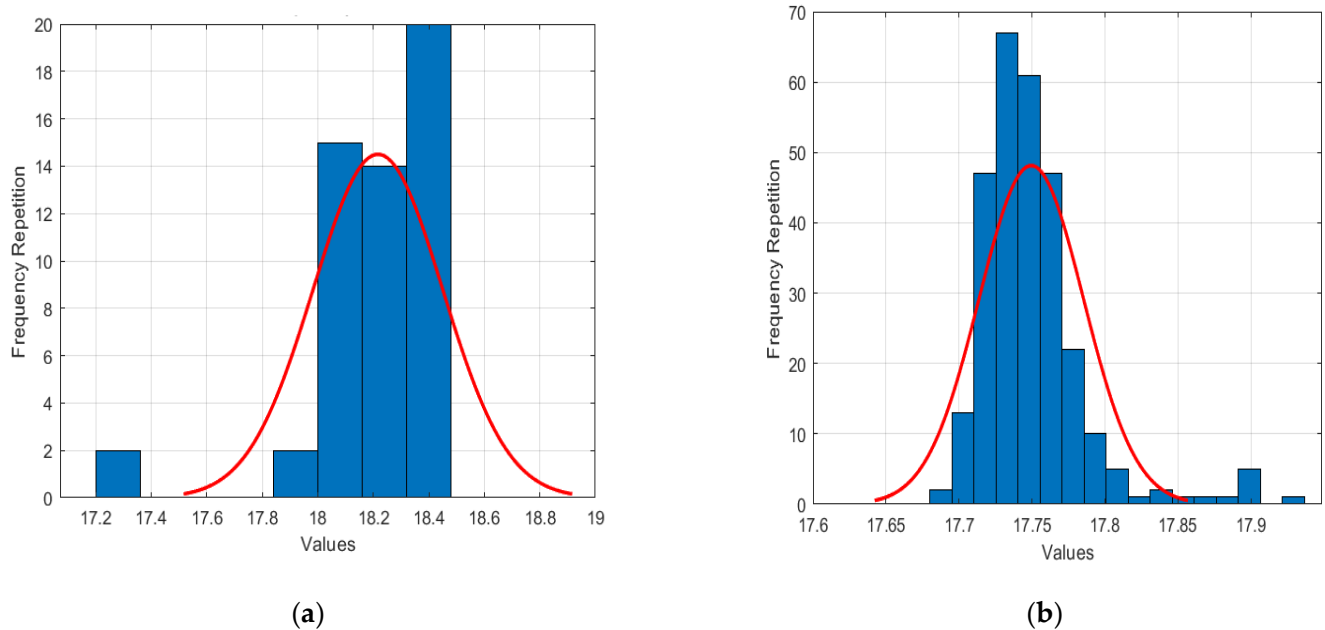


Figure 9. Probability histogram for the capacitance measurements obtained from Figure 2. (a) Inside the cage. (b) Outside the cage.

These results suggest that the presence of the Faraday cage may influence the distribution of the data. A negative skewness inside the cage could indicate a higher concentration of low values, while a positive skewness outside the cage might suggest a higher concentration of high values. This analysis reinforces the importance of considering the influence of the environment, in this case, the presence of the Faraday cage, when interpreting the statistical characteristics of the time series.

3.4. Periodograms

The previous results are complemented below by comparing the periodogram variability both inside and outside the shield. It can be seen in all the figures that when the photomultiplier is inside the box, the residual or random components are considerably attenuated in the frequency spectrum, which is not the case when the periodograms of the measurements outside the box are obtained.

In Figure 10a,b, respectively, it can be seen that the frequencies are more stable with a tendency toward a flat spectrum starting from component 0.1. The rest of the graph in Figure 11 are illustrated with more ripple and instability, which induces more asymmetry in the distribution of the data in the frequency spectrum.

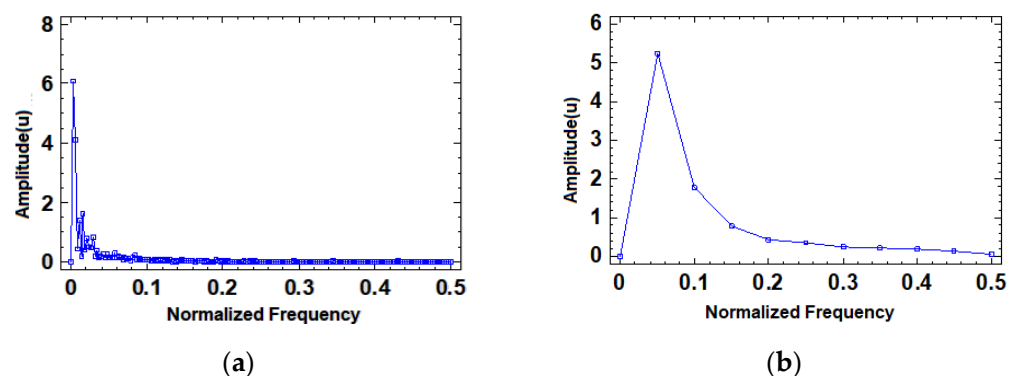


Figure 10. Periodogram for (a) capacitance ultra-stable capacitor outside the box; (b) capacitance ultra-stable capacitor inside the box.

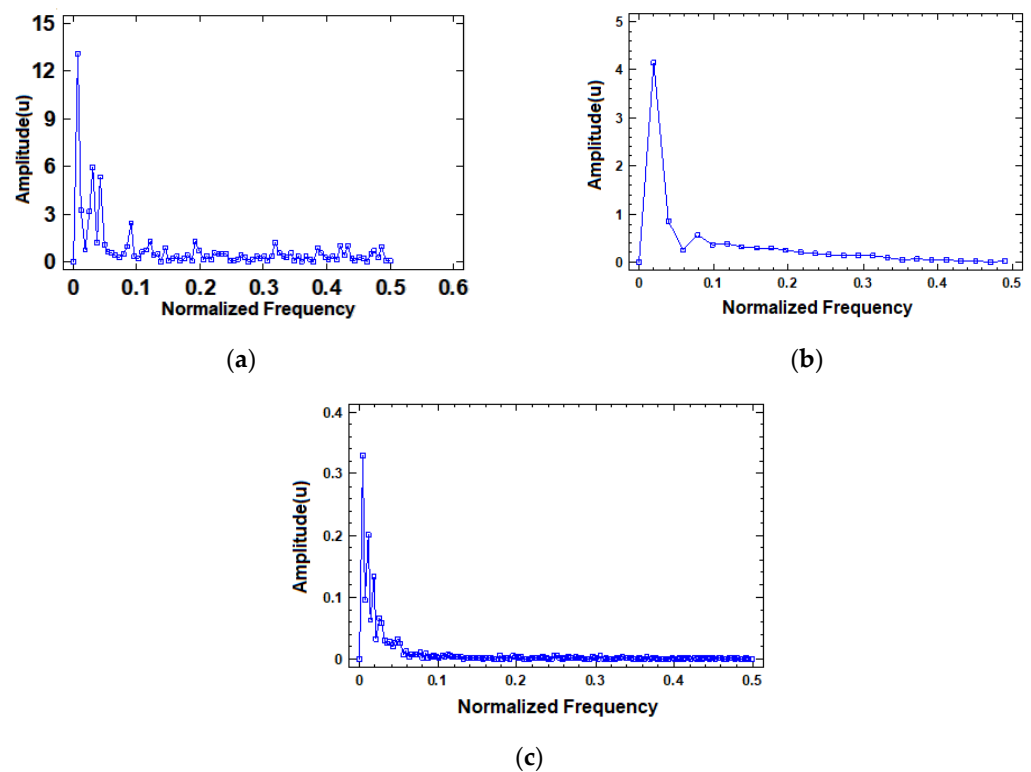


Figure 11. Periodogram for (a) capacitor outside the cage, (b) photomultiplier capacitance between anode and cathode inside the enclosure, and (c) photomultiplier extracted from the box.

4. Discussion

In the first experiment corresponding to the capacitance measurements between April and September 2020, it was found, as expected, that there was no correlation between C_p and the other environmental parameters outside the MFC, but correlations were found within it, the highest being the one between C_p and D_{cx} . However, the change was much smaller than in previous trials. One can hypothesize that these changes were small due to the different setups and to the varying environmental conditions, i.e., much less variability of D_{cx} , N , different humidity values, and a minimum of solar activity.

Regarding the humidity values, it must be stressed that they were measured outdoors in the lab. These values could be very different from those inside the lab and inside the cage, and thus, its usefulness can be doubted.

Additionally, it was remarkable the change in the distribution of power into frequency components in the periodogram of the capacitance measurements (when inside and outside the MFC).

Since there was noticeable variability in the results, and since RH was not measured inside the box, it was concluded that more experiments are needed to understand the underlying reason behind those differences.

On the other hand, in the second experiment, analysis of the measurements in a photomultiplier inside an MFC was performed, and it could be observed that the capacitance between the anode and the cathode of a photomultiplier behaved similarly to the capacitance of the ultra-stable capacitor analyzed in [1] when measured inside an interleaving structure. This means that both capacitances fluctuate when placed inside the cavity, but they recover their design values when extracted from the box(es). Some remarkable facts are (a) the capacitances recover their design values not immediately but after a certain time, which can be about 24 h; and (b) the confidence intervals of the means change significantly (in the presented case) from inside to outside the enclosure (in the case of the ultra-stable capacitor, it increased from 0.004 to 0.008 nF).

Regarding the correlations between capacitances C_{PMT} and the other variables, they were found in different circumstances: (a) only between C_{PMT} and D_{cx} when the jump of C_{PMT} took place and when the jump was included in the analysis, (b) only between C_{PMT} and N when the jump was excluded from the analysis, and (c) a multiple regression analysis yield a slight correlation between C_{PMT} and both D_{cx} and N .

The variability experienced by different devices like the ultra-stable capacitor and the circuitry of a photomultiplier tube is also verified by different periodograms that are generated inside and outside the cavity.

Regarding the analysis of asymmetry, the results presented in Table 2 illustrate the following patterns: Within the enclosure, the negative skewness value (-2.2168) indicates that the left tail of the distribution is longer or heavier compared to the right tail. Conversely, outside the enclosure, the positive value (2.1978) suggests that the right tail of the distribution is longer or heavier than the left tail. This asymmetry can provide relevant information about the structure of the data under analysis, and periodogram analysis can aid in identifying and better understanding the characteristics and frequency components present in the data.

5. Conclusions

In this paper, it is shown in experiment E.I that the capacitance of an ultra-stable capacitor changes inside an MFC, but this change seems to be correlated with some environmental variables. In the current case, a correlation was found to exist between C_p and D_{cx} . Since the used RH values were the ones outside the box (and outdoors), they could not be assessed its importance in a correlation analysis (contrary to what happened in [9]).

The periodograms of the capacitance measurements changed significantly when their location changed from outside to inside the shield. In experiment E.II, when analyzing the capacitance between the anode and cathode of a PMT, a slight correlation between the capacitance and some environmental variables were found. The periodograms changed significantly, and a lag effect was observed when the DUTs were extracted from the enclosures.

The utilization of the periodogram for dissecting data variability by frequency renders it a valuable tool for analyzing and gaining deeper insights into the inherent patterns and variations both within and outside the MFC. Additionally, we conducted asymmetry analyses using the skewness coefficient to quantify and assess the extent of asymmetry in the data distributions obtained within and beyond the MFC.

Author Contributions: Conceptualization, V.M.-S., M.E.I.-M. and P.F.d.C.; methodology, J.G.C. and E.B.O.; software, F.M.M.-P. and J.C.C.-P.; validation, M.E.I.-M. and P.F.d.C.; formal analysis, S.S. and M.E.I.-M.; investigation, E.B.O. and V.M.-S.; resources, P.F.d.C. and M.E.I.-M.; data curation, F.M.M.-P., J.A.M., S.S. and J.G.C.; writing—original draft preparation, V.M.-S., M.E.I.-M. and P.F.d.C.; writing—review and editing, M.E.I.-M. and P.F.d.C.; visualization, F.M.M.-P. and J.G.C.; supervision, V.M.-S., J.A.M. and P.F.d.C. All authors have read and agreed to the published version of the manuscript.

Funding: Miguel E. Iglesias Martínez's work was partially supported by the postdoctoral research scholarship "Ayudas para la recualificación del sistema universitario español 2021–2023. Modalidad: Margarita Salas" from the Ministerio de Universidades, Spain, funded by the European Union-Next Generation EU and additionally funded by "Ayuda para potenciar la investigación postdoctoral de la UPV (PAID-PD-22)". The work of S.S. is partially supported by DGAPA-UNAM (México) Project No. IN103522. This work was supported by the Spanish Ministerio de Ciencia e Innovación (PID2022-142407NB-I00) and by Generalitat Valenciana (grant CIPROM/2022/30), Spain. F.M.M.P also acknowledges the financial support from the Universitat Politècnica de València (PAID-01-20-25), Spain. This work was supported by the Spanish government (PID2021-128676OB-I00 and PID2022-142407NB-I00) and by Generalitat Valenciana (grant CIPROM/2022/30), Spain.

Data Availability Statement: Data are contained within the article.

Conflicts of Interest: The authors declare no conflict of interest.

References

1. Milián-Sánchez, V.; Mocholí-Salcedo, A.; Milián, C.; Kolombet, V.A.; Verdú, G. Anomalous effects on radiation detectors and capacitance measurements inside a modified Faraday cage. *Nucl. Instrum. Methods Phys. Res. A* **2016**, *828*, 210–228. [[CrossRef](#)]
2. Amin, M.S.; Peterson, T.F.; Zahn, M. Advanced Faraday cage measurements of charge and open-circuit voltage using water dielectrics. *J. Electrostat.* **2006**, *64*, 424–430. [[CrossRef](#)]
3. Glasscott, M.W.; Brown, E.W.; Dorsey, K.; Laber, C.H.; Conley, K.; Ray, J.D.; Moores, L.C.; Netchaev, A. Selecting an Optimal Faraday Cage To Minimize Noise in Electrochemical Experiments. *Anal. Chem.* **2022**, *94*, 11983–11989. [[CrossRef](#)] [[PubMed](#)]
4. Tran, D.; Dutoit, F.; Najdenovska, E.; Wallbridge, N.; Plummer, C.; Mazza, M.; Raileanu, L.E.; Camps, C. Electrophysiological assessment of plant status outside a Faraday cage using supervised machine learning. *Sci. Rep.* **2019**, *9*, 17073. [[CrossRef](#)] [[PubMed](#)]
5. Milián-Sánchez, V.; Scholkmann, F.; de Córdoba, P.F.; Mocholí-Salcedo, A.; Mocholí, F.; Iglesias-Martínez, M.E.; Castro-Palacio, J.C.; Kolombet, V.A.; Panchelyuga, V.A.; Verdú, G. Fluctuations in measured radioactive decay rates inside a modified Faraday cage: Correlations with space weather. *Sci. Rep.* **2020**, *10*, 8525. [[CrossRef](#)]
6. Pireddu, G.; Rotenberg, B. Frequency-Dependent Impedance of Nanocapacitors from Electrode Charge Fluctuations as a Probe of Electrolyte Dynamics. *Phys. Rev. Lett.* **2023**, *130*, 098001. [[CrossRef](#)]
7. Güneşer, M.T.; Elamen, H.; Badali, Y.; Altındal, Ş. Frequency dependent electrical and dielectric properties of the Au/(RuO₂:PVC)/n-Si (MPS) structures. *Phys. B Condens. Matter* **2023**, *657*, 414791. [[CrossRef](#)]
8. Kolahian, P.; Grimm, F.; Baghdadi, M. A Comprehensive Review on Planar Magnetics and the Structures to Reduce the Parasitic Elements and Improve Efficiency. *Energies* **2023**, *16*, 3254. [[CrossRef](#)]
9. Pommé, S.; Pelczar, K. On the recent claim of correlation between radioactive decay rates and space weather. *Eur. Phys. J. C* **2020**, *80*, 1093. [[CrossRef](#)]
10. Pommé, S.; Pelczar, K. Role of ambient humidity underestimated in research on correlation between radioactive decay rates and space weather. *Sci. Rep.* **2022**, *12*, 2527. [[CrossRef](#)]
11. Milián-Sánchez, V.; Iglesias-Martínez, M.E.; Scholkmann, F.; Fernández de Córdoba, P.; Castro-Palacio, J.C.; Sahu, S.; Panchelyuga, V.A. Reply to: Role of ambient humidity underestimated in research on correlation between radioactive decay rates and space weather. *Sci. Rep.* **2022**, *12*, 2530. [[CrossRef](#)] [[PubMed](#)]
12. Mocholí, A.; Mocholí, F.; Milián-Sánchez, V.; Guerra-Carmenate, J.; Iglesias-Martínez, M.E.; de Córdoba, P.F.; Castro-Palacio, J.C.; Sahu, S.; Monsoriu, J.A.; Lorduy, M.; et al. Variability of coil inductance measurements inside an interleaving structure. *Sci. Rep.* **2022**, *12*, 16272. [[CrossRef](#)] [[PubMed](#)]
13. Anderson, J.L.; Spangler, G.W. Serial statistics: Is radioactive decay random? *Phys. Chem. J.* **1973**, *77*, 3114–3121. [[CrossRef](#)]
14. Anderson, J.L. Non-Poisson Distributions Observed during Counting of Certain Carbon-14-Labeled Organic (Sub)Monolayers. *J. Phys. Chem.* **1972**, *76*, 3603–3612. [[CrossRef](#)]
15. Emery, G.T. Perturbation of Nuclear Decay Rates. *Annu. Rev. Nucl. Part. Sci.* **1972**, *22*, 165–202. [[CrossRef](#)]
16. Jenkins, J.H.; Herminghuysen, K.R.; Blue, T.E.; Fischbach, E.; Javorsek, D.; Kauffman, A.C.; Mundy, D.W.; Sturrock, P.A.; Talnagi, J.W. Additional experimental evidence for a solar influence on nuclear decay rates. *Astropart. Phys.* **2012**, *37*, 81–88. [[CrossRef](#)]
17. Barnes, V.E.; Bernstein, D.J.; Bryan, C.D.; Cinko, N.; Deichert, G.G.; Gruenwald, J.T.; Heim, J.M.; Kaplan, H.B.; LaZur, R.; Neff, D.; et al. Upper limits on perturbations of nuclear decay rates induced by reactor electron antineutrinos. *Appl. Radiat. Isot.* **2019**, *149*, 182–199. [[CrossRef](#)]
18. Guo, F.; Lv, H.; Wu, X.; Yuan, X.; Liu, L.; Ye, J.; Wang, T.; Fu, L.; Wu, Y. A machine learning method for prediction of remaining useful life of supercapacitors with multi-stage modification. *J. Energy Storage* **2023**, *73 Pt D*, 109160. [[CrossRef](#)]
19. Acar, Z.; Nguyen, P.; Cui, X.; Lau, K.C. Room temperature ionic liquids viscosity prediction from deep-learning models. *Energy Mater.* **2023**, *3*, 300039. [[CrossRef](#)]
20. Guo, F.; Wu, X.; Liu, L.; Ye, J.; Wang, T.; Fu, L.; Wu, Y. Prediction of remaining useful life and state of health of lithium batteries based on time series feature and Savitzky-Golay filter combined with gated recurrent unit neural network. *Energy* **2023**, *270*, 126880. [[CrossRef](#)]
21. Cao, W.; Zhong, Q.; Li, H.; Liang, S. A Novel Approach for Associative Classification Based on Information Entropy of Frequent Attribute Set. *IEEE Access* **2020**, *8*, 140181–140193. [[CrossRef](#)]
22. Tang, H.; Zhang, Y.-Y.; Zheng, S.-X.; Song, X.-F. Sampling optimization for 3D surface measurement. Part II: Sampling interval optimization based on cumulative power spectral density analysis. *Measurement* **2022**, *200*, 111692. [[CrossRef](#)]

Disclaimer/Publisher’s Note: The statements, opinions and data contained in all publications are solely those of the individual author(s) and contributor(s) and not of MDPI and/or the editor(s). MDPI and/or the editor(s) disclaim responsibility for any injury to people or property resulting from any ideas, methods, instructions or products referred to in the content.